Accepted Manuscript

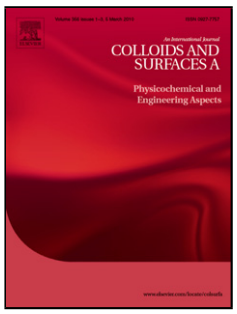

Title: Filling gaps in the knowledge of melittin on lipid membranes

Authors: María José Elías Tissera, E. Aníbal Disalvo, M. Florencia Martini, Andrea C. Cutró

PII: S0927-7757(18)30920-8
DOI: https://doi.org/10.1016/j.colsurfa.2018.10.055
Reference: COLSUA 22941

To appear in: *Colloids and Surfaces A: Physicochem. Eng. Aspects*

Received date: 11-9-2018
Revised date: 17-10-2018
Accepted date: 21-10-2018

Please cite this article as: Tissera MJE, Disalvo EA, Martini MF, Cutró AC, Filling gaps in the knowledge of melittin on lipid membranes, *Colloids and Surfaces A: Physicochemical and Engineering Aspects* (2018), https://doi.org/10.1016/j.colsurfa.2018.10.055

Filling gaps in the knowledge of melittin on lipid membranes

María José Elías Tissera[1], E. Aníbal Disalvo[1], M. Florencia Martini[2,3]*and Andrea C. Cutró[1]*

[1.] *Laboratorio de Biointerfases y Sistemas Biomimeticos. CITSE-UNSE-CONICET. Ruta Nacional 9, Km. 1125, 4206. Villa el Zanjón, Santiago del Estero, Argentina.*

[2.] *Cátedra de Química Medicinal, Facultad de Farmacia y Bioquímica, Universidad de Buenos Aires (UBA), Junín 956, Ciudad Autónoma de Buenos Aires (1113), Argentina*

[3.] *CONICET- Universidad de Buenos Aires. Instituto de la Química y Metabolismo del Fármaco (IQUIMEFA). Ciudad Autónoma de Buenos Aires, Argentina*

***Dr M. Florencia Martini**, Cátedra de Química Medicinal, Facultad de Farmacia y Bioquímica, Universidad de Buenos Aires (UBA), Junín 956 PP, CABA (1113), Argentina. flormartini1@gmail.com

Dr. Andrea C. Cutró, Laboratorio de Biointerfases y Sistemas Biomimeticos. CITSE-UNSE-CONICET. Ruta Nacional 9, Km. 1125, 4206. Villa el Zanjón, Santiago del Estero, Argentina. cutro.andrea@gmail.com

Graphical abstract

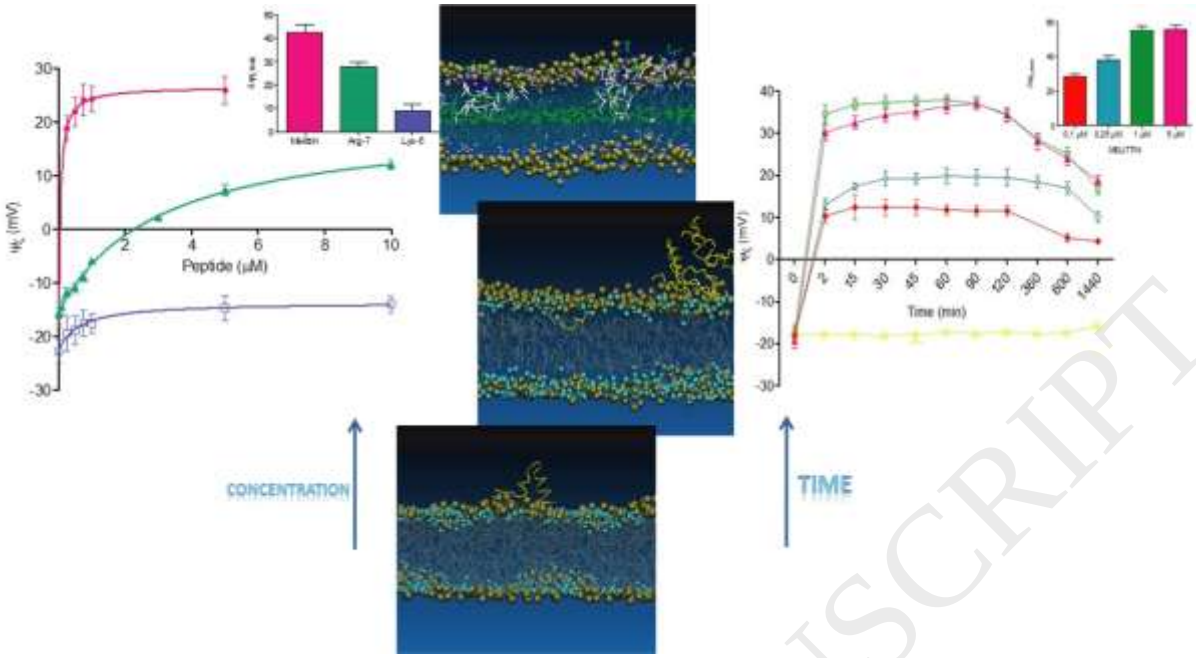

Highlights

- Not everything has been said about the mechanism of action of melittin
- Melittin has the ability to penetrate the zwitterionic lipid membranes under the right conditions
- The existence of defects in a membrane favors the penetration of melittin
- The penetration of melittin favors the increase of membrane defects

ABSTRACT

Melittin (ML) is a small peptide of 26 residues rich in arginine (Arg) and lysine (Lys). Several studies have been done to understand the mechanism of interaction with neutral and negatively charged lipids. However, it is not known with certainty how this interaction depends on the electrostatic or hydrophobic forces according to the composition of the membrane, nor with the different organization of lipids on the membrane, such as the microdomains that could take place in it. Therefore, comparative studies of the interaction and the effect of ML with respect to cationic peptides (Arg-7 and Lys-5) were conducted to get a deeper insight of the ML interaction mechanism with membranes. In this regard, measurements of zeta potential of different model membranes (DOPC, DMPC and DMPE liposomes) in the presence of the peptides, and molecular dynamics simulations were

performed. In the special case of DMPC, we worked in its gel like-ripple phase, in order to analyzed defects of packing that potentially expose hydrocarbon regions.
In relation with experimental results, molecular analysis of ML interaction with zwiterionic lipid membrane in its ripple phase was performed by unbiased molecular dynamics simulations.
The results allow us to remark that ML penetration is favored in the gel-liquid crystalline phase transition in zwitterionic lipids. The importance of this study lies in the understanding of the first stages of action of the ML in eukaryotic membranes, in model systems of its main lipid composition.

Keywords: MELITTIN; MELITTIN-LIPID MEMBRANE INTERACTION; LIPID COMPOSITION; LIPID ORGANIZATION; ZETA POTENTIAL; MOLECULAR DYNAMIC SIMULATIONS

1. Introduction

The bee venom or apitoxin, isolated from the European honeybee Apismellifera, has been widely used for the treatment of inflammatory diseases such as arthrosis, rheumatoid arthritis, among others [1,2] since ancient times in traditional medicine. Apitoxin is constituted by peptides, enzymes and amines; being melittin the main component because represents the 50% of the dry weight of the bee venom [3]. Melittin (ML) is a cationic, small peptide composed of 26 amino acid residues [(+)Gly-Ile-Gly-Ala-Val-Leu-Lys(+)-Val-Leu-Thr-Thr-Gly-Leu-Pro-Ala-Leu-Ile-Ser-Trp-Ile-Lys(+)-Arg(+)-Lys(+)-Arg(+)-Gln-Gln-NH2] in which the N-terminal region is predominantly hydrophobic whereas the C-terminal region is hydrophilic due to the presence of a section of positively charged amino acids [4-8].

There is extensive evidence that ML has a cytolytic effect in different biological membrane models. For example, its interaction with red cells has shown to produce hemolysis [9,10]. Similar effects were observed in bacterial membranes, cancer cells, leucocytes, mitochondrial membranes and even artificial lipid membranes [7,9-13].

In order to explain its action, different models of interaction between this peptide and membranes have been proposed, such as carpet, detergent and formation of toroidal or barrel pores in the lipid bilayer [14-17]. In particular, Hristova et al. [18], working on dioleoyl-phosphatidylcholine (DOPC) membranes with oriented circular dichroism show that the tilt angle of bilayer-bound ML is perpendicular to the membrane normal, suggesting that ML peptides are laying on the membrane surface. In the same work, X-ray diffraction experiments of ML, containing DOPC lipid films deposited on quartz slides, show that ML does not penetrate the hydrophobic core of the membrane, but instead resides in the membrane interface at the height of the glycerol-carbonyl groups [18].

Based on other works of ML- zwiterionic lipid membranes [7,19-22] the average molecular mechanism of toxicity, is thought to take place in this sequence: 1. membrane binding and helix formation, 2. ML aggregation in the membrane interphase, and 3. transient pore formation. However, molecular details of each step and its dependence with membrane organization have not been analyzed in depth.

On the other hand, different works suggest that the action of ML on bilayers depends on factors such as: the composition of the membrane, temperature, pH, and the concentration of the peptides [23-25]. It has been shown that ML strongly binds to both zwitterionic and negatively charged phospholipid membranes, but by means of different mechanism. At first glance, it seems to form transmembrane pores in zwitterionic lipid bilayers via a barrel-stave mechanism and as a detergent in negatively charged membranes [26,27]. However, other authors state that these theories are not consistent with the mechanism of action of ML and they propose the toroidal model as a mechanism of pore formation, where ML is always associated with lipid head groups even when inserted perpendicularly into the lipid bilayer. If this is so, the pore would be coated by both the peptides and the lipid head groups [19,28]. In addition to that, in the first step by which ML form a pore, the peptide needs to be accumulated on the membrane surface and then insert into the membrane. This transition is associated to changes in the local concentration of the peptide. At low concentration, ML tends to reach membrane interphase in a parallel orientation, when the concentration is

increased up to a critical value; it acquires a transmembrane (TM) orientation [21,29].

Another study revealed that since ML carries high cationic (+6) charges at neutral pH, and interacts strongly with the lipid head groups, the reorientation from parallel to TM is very expensive in terms of energy and may not be feasible [15,30].

Therefore, it is not yet clear how the first molecular steps by which ML associates with the membrane takes place and what other complex structures may be formed. This could be due because in most computational molecular approaches, external forces are used to induce the formation of the pore, e.g. the use of potential of mean force [31], or positioning of the peptides inside the membrane, bypassing the step by which ML penetrates into the membrane [32]. Thus, the question of how the interaction of ML with membranes takes place in terms of the role of ML charges and structural properties of the membrane is relevant.

In 2013, Santo et al. [33] performed a coarse-grained simulation (CG) using the MARTINI force field and observed how ML formed transient pores in phosphatidylcholine membranes: phosphatidylglycerol (PC: PG). Pores were formed when 3-5 peptides had been assembled and there is not essential the reorientation of all normal peptides to the surface of the membrane; many of them had their terminal residues anchored to the same monolayer, and these peptides assumed bent U-shaped conformations. Other studies of the interaction of ML with model membranes as DMPC, in which the lipid bilayer was thin enough to be traversed by an ML molecule, the penetration of the peptide was not observed under the studied conditions [34].

Phosphatidylcholine membranes are studied as model lipid membranes of mammalian cells, mainly because it is the most abundant phospholipid in the membranes of this type of cells [35,36]. The saturated diacyl phosphatidylcholines are characterized to show a pre-transition between the L_β and P_β phase and a transition phase between the P_β and the L_α phase. The P_β phase is known as the ripple phase which is considered to be one-dimensional defects of fluid lipid molecules [37]. Specifically, hydrophobic interactions take place in defects of packing that expose hydrocarbon regions, frequently found in membranes presenting spontaneous curvature such as ripple regions or protrusion according with the head group chemical structure [38,39]. There, a particular organization of carbonyl groups and water has been suggested. There are works in bibliography which get deep inside peptide-membrane interaction in relation to lipid phases with packaging defects [40]. Since, as states above ML resides in the membrane interface at the height of the glycerol-carbonyl groups [18] it would be of interest to explore the affinity of ML for this phase state.

In addition, as ML contains a significant amount of positively charged amino acid, the role of charges in this interaction deserves more attention.

For these reason, here, we analyze the interaction of ML with model mammalian lipid membranes, analyzing changes in its surface properties, in comparison to peptides containing only positively charged amino acids such as pentalysine (Lys-5) and heptarginine (Arg-7) and following a molecular approach through molecular dynamics simulations, long enough to regard changes without external forces or bypassing any step of the interaction. We also analyzed different phase states of the phospholipids bilayers, including and focusing on the ripple phase, where the defects could enhance the possibility of ML penetration. The

objective of this work is to understand the process by which melittin alters eukaryotic lipid membranes, taking into account the organization and packaging of lipids.

2. Materials and Methods

2.1. Chemicals

1,2-Dimyristoyl-sn-glycero-3-phosphocholine (DMPC; >99% purity), 1,2-dimyristoyl-sn-glycero-3-phosphoethanolamine (DMPE; >99% purity) and 1,2-dioleoyl-sn-glycero-3-phosphocholine (DOPC, >99% purity) were obtained from Avanti Polar Lipids, Inc. (Alabaster, AL). Potential peroxidation of lipids was checked by FTIR and UV spectroscopies. Melittin, hepta-Arginine (Arg-7) and penta-Lysine (Lys-5) were purchased from Sigma–Aldrich (Saint Louis, MO). Chloroform, methanol and KCl were of analytical grade. All aqueous solutions were prepared with ultrapure water obtained from an Osmion reverse osmosis system containing two carbon and two ion-exchange columns. Then, water was purified through a 0.22 m Zetapore filter. The resistivity of the purified water was 18 MΩ.cm.

2.2. Liposome preparation

The stock solutions of DMPC, DMPE and DOPC were prepared by dissolving a weighted amount of solid lipid in mixture of chloroform: methanol (3:1) up to reach a final concentration of 4 mM. Aliquots of each stock solution were used to prepare a lipid films by slow evaporation of the organic solvent with a nitrogen stream in a glass tube with conical base. The residual organic solvent was removed under vacuum. In order to obtain a multilamellar vesicle suspension (MLVs), the dried film was hydrated in 1 mM KCl aqueous solution at pH=5.0 above the phase transition temperature of the lipids, for 60 min [41,42].

2.3. Liposome Quantification

Phospholipid concentration was determined by quantifying inorganic phosphorus in samples mineralized essentially [43]. The inorganic phosphate concentration was colorimetrically determined according to Chen et al. [44] as described by Ames [45].

2.4. Zeta potential

The Zeta potentials (ψ_ζ) of DMPC, DMPE and DOPC liposomes were determined in Zeta-Meter System 3.0 equipment, at 18 ± 2°C. The voltage was fixed at 75 V. The total lipid concentration in all cases was 52 µM. Once prepared, liposomes were cooled down to 18°C and incubated at that temperature with different peptide concentrations (1–10 µM) during 1 h. A total of 20 measurements were carried out focusing different particles for each sample. Data reported are the average of the measurements done for each condition with, at least, three different batches of liposomes. The Zeta potential values obtained were used to estimate the degree of coverage (θ) for each peptide, Equation (1):

$$\theta = \frac{\zeta_0 - \zeta}{\zeta_0 - \zeta_{max}} \quad (1)$$

Where $\boldsymbol{\zeta_0}$ is the zeta potential of the liposome in the absence of peptide; $\boldsymbol{\zeta_{max}}$ is the zeta potential value for liposomes saturated with peptide and $\boldsymbol{\zeta}$ is the zeta potential at any

intermediate peptide concentration.

When $\zeta = \zeta_0$, $\theta = 0$ and when $\zeta = \zeta_{max}$, $\theta = 1$

2.4.1 Kinetics measurements of Zeta Potential

The changes of DMPC Zeta Potential as a function of time were measured in a Zeta-Meter System 3.0 equipment, at 18 ± 2°C; the voltage was fixed at 75 V. The DMPC liposomes were incubated with a fixed ML concentration (0,1; 0,25; 1 and 5 μM, respectively) at different time up to 24 h. A total of 20 measurements were carried out focusing different particles for each sample. Data reported are the average of the measurements done. The zeta potential values obtained were represented as a function of time in order to evaluate the effect on the zeta potential kinetic behaviour by the action ML.

2.5. Computer setup for MD simulations

We have performed united atom (UA) scale MD simulations of zwitterionic DMPC lipid bilayers in aqueous solution of ML or Lys-5 in each case.

The simulated systems consist of a periodically replicated cell of 60 x 60 x 80 $Å^3$, containing 64 molecules of phospholipid DMPC in each leaflet (128 in total) and 1 ML or 1 Lys-5, depending on the case, solvated with ~ 6000 molecules of water and Cl^- as counter-ion, in sufficient quantity to reach a neutral system. The systems are effectively periodic in 3D.

In order to analyze the collective interaction of ML in the interaction with the lipid membrane, we perform atomistic systems in cells of 98 x 98 x 140 $Å^3$ of 338 lipids, ~12000 molecules of water and 7 melittins (Cl^- as counter-ion, in order to reach a neutral system).

As we have cited in the introduction section, the studied pore formation by ML depends on several parameters, one of the most important is the peptide/lipid (P/L) ratio. In several studies, it is reported that ML induces pore formation only when the threshold ratio between P/L is above 1/60 [21,46-48]. In our case, we use a P/L of 1/128 as the lowest value and 1/48, for the relationship that we assume as a potential concentration for pore formation.

The MD simulations were performed by GROMACS 5.0 software package [49-55]. Coordinates of ML were retrieved from the protein data bank (PDB ID: 2MLT) in α-helical conformation (www.rcsb.org). ML, Lys-5 and DMPC were described by GROMOS-96 53a6 united atom force field [56,57]. The united atom force field of Berger et al. [58] was applied for the phospholipids. Water was modeled using the simple point charge (SPC) model [59]. The electrostatic interactions were handled with the smooth particle mesh Ewald (SPME) version of the Ewald sums [60,61]. In all the simulations, the van der Waals interactions were cutoff at 1.5 nm. The simulations were carried out in the NPT ensemble using the Nose-Hoover thermostat. The whole system was coupled to a temperature bath with a reference temperature of 291 K, in accordance with the experimental settings. The barostat used was Parrinello-Rahman in a semi isotropic perform, where uniform scaling of x-y box vectors, independent of z, was set at a pressure of 1 atm. All bond lengths of the molecules were constrained using the LINCS algorithm. The time step for the integration of the equation of motion was 2 fs.

The systems of 1 peptide:128 DMPC was minimized and equilibrate. MD simulations were carried out up to 300 ns production run after the equilibration of the system. Those MD simulations performed with 7 ML:338 DMPC in water were carried out up to 600 ns production run after the equilibration of the system.

On the other hand, with the aim to reach longer simulation times of the UA system, we worked with a coarse grain model, using the Martini force field. The system was validated for the interaction of a ML with DMPC membrane (1:128), under similar conditions of the previous system. Then, we performed the interaction of 7 ML with DMPC membrane. The system was assembled using Martini v 2.2 [62-65] and the DMPC was built evaluating the DLPC and DPPC's coarse grain models [66] of the cited force field. The membrane was equilibrated before adding the corresponding ML peptide/s, and was in accordance with the properties obtained by Vries et al (2005) [67] for the CG model of ripple phase. The validation system was run 1 μs, while the system of 7 ML with a bilayer of DMPC was run for 105 μs (7 ML peptides, 338 DMPC and 5258 W beads), under similar conditions to those proposed in the experimental and UA model. The working ensemble was $NP_{xy}P_zT$.

To compare the results of these simulations with the properties of DMPC membrane in the absence of peptides, we also performed a CG simulation for DMPC bilayer for a time period of 10 μs.

We analyzed visually the simulated trajectories through the VMD software, as well as obtained snapshots of the most representative initial and final stages. On the other hand, for a quantitative analysis, the evaluated properties were analyzed with the tools package of software Gromacs, in the different periods of the trajectory, reported in Results.

The evaluated properties were: the electronic density profile (EDP) to know the order of our systems in the plane normal to the membrane; the formation of H bonds between the studied peptides and the lipid membrane, as a function of the simulated time; the interaction energy between peptide-DMPC membrane; the radial distribution function between the O of the phospholipid phosphate groups and the center of mass of the charged residues of the peptides studied; the order parameter of the hydrocarbon tails of the phospholipids. All these properties are duly detailed in the Results section.

Likewise, we evaluated the number of waters in the interior plane of the membrane, with a thickness of 6 Å, 3 Å towards + z and 3 Å towards -z, with respect to the midpoint of the lipid bilayer. To carry out this analysis, we previously centre the lipid bilayer on z in the trajectories.

Once this was done, the trajectory of the P atoms (of the phosphate groups) of each monolayer was analyzed, in order to evaluate the permanence of the middle point of the bilayer in a plane of z. Once the mean point in z (PMz) was known, the number of existing waters in the box was evaluated, between the planes comprised between PMz +3; PMz-3. The results of this analysis are duly detailed in the Results section.

The figures of MD simulations were done with VMD [68] and Grace (http://plasma-gate.weizmann.ac.il/Grace/) software.

3. Results and Discussion

Interaction of melittin with liposomes of different lipid composition

We analyzed the interaction of ML with phospholipid membranes by the effect of this peptide on the zeta potential of DOPC, DMPC and DMPE liposomes at 18ºC. ML shifts the negative zeta potential of the membranes to positive values in all the cases (Figure 1). This effect is higher when the values of initial potential are more negatives (insert Figure 1). The highest change in zeta potential was observed for DMPE liposomes in relation with PC liposomes. Besides, DOPC and DMPC did not show significant differences. These results could indicate that ML interacts with lipid membrane and its basic amino acids are more exposed in the surface of DMPE liposomes than PC liposomes. In order to better understand the electrical effect of ML on membrane, the degree of coverage and the apparent dissociation constant of ML for each phospholipid membranes were determined from the zeta potential values as described in Material and Methods.

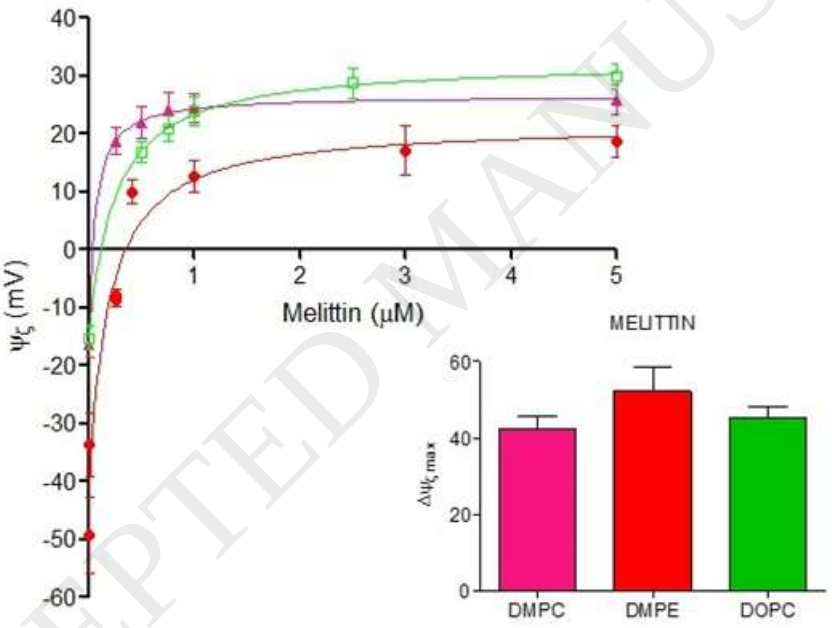

Figure 1. *Effect of peptide ML on zeta potential of DMPC (▲), DMPE (●) and DOPC (□) liposomes, measured after 60 min incubation. Change of zeta potential produced by different ML concentration.*

Insert at bottom: Maximal change produced by ML on DMPC, DMPE and DOPC liposomes zeta potential.

The binding of ML with the lipid membranes exhibited a Langmuir behavior, independently of the lipid composition, indicating that ML is bound to independent and equivalent sites into the membrane (Figure 2).

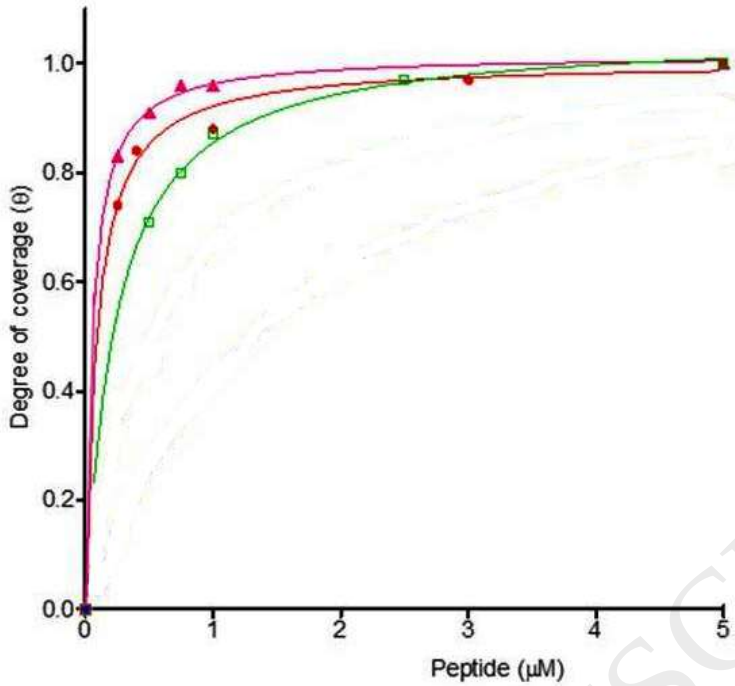

Figure 2. *Adsorption isotherms for MLV of different phospholipid composition. ML-DMPC (▲), ML-DMPE (●), ML-DOPC (□)*

Although the maximum change in zeta potential takes place in DMPE liposomes, the apparent affinity of ML is higher for DMPC in comparison with DMPE (Table 1). This result is in good agreement with the interphospholipid interaction of DMPE [69,70], which result in a good surface to interact but difficult to penetrate the membrane [71,72]. In this case, DMPE is in a gel state, which also diminishes the possibility of peptides penetration.

Table 1. *Apparent constant dissociation of ML for MLV of DMPC, DMPE and DOPC at 18ºC*

Lipid	Kd_{app} (μM)	R^2
ML DMPC	0.05 ± 0.01	0.9997
ML DMPE	0.09 ± 0.01	0.9980
ML DOPC	0.24 ± 0.01	0.9994

The difference between the Kd_{app} of the different PCs membranes, interacting with ML, may be related to the difference in phase state, since at 18ºC, DOPC is in the crystalline liquid state and DMPC in the ripple phase. In the latter, there is an increase in defects in the membrane, which may favor the penetration of the peptides. This result could be in agreement with Upadhyay et al [34] in the sense that they could not obtain ML penetration in DMPC membrane in the liquid crystalline state.

Taking these results into account, we decided to study the interaction of ML with the main zwitterionic lipid of eukaryotic cells, as is the case of phosphatidylcholine, in its ripple phase. This undulated phase was previously studied in biological relevant processes as: spontaneous curvature, microdomain segregation in cellular membrane, and even penetration of peptides [38,39].

Comparison of the interaction of melittin and cationic peptides with DMPC membranes in its ripple phase

ML has a net charge of +6, arising from a protonated N-terminus (NH_3^+) with an amidate C-terminal, 3 lysine (LYS) and 2 arginine (ARG) residues. In order to evaluate the contribution of the charges of these amino acids [ML total charge: +6 at pH=5] on the interaction of the peptide with DMPC lipid membranes at 18ºC, the effect of ML on the zeta potential of the membrane was compared with the effect observed with polypeptides of Arg-7 (total charge: +7) and Lys-5 (total charge: +5). The results obtained show a significant differential effect of ML. Although both ML and Arg-7 produce a shift to positive potential values in contrast to Lys-5 (Figure 3) ML shows a net displacement to positive value at very low concentrations.

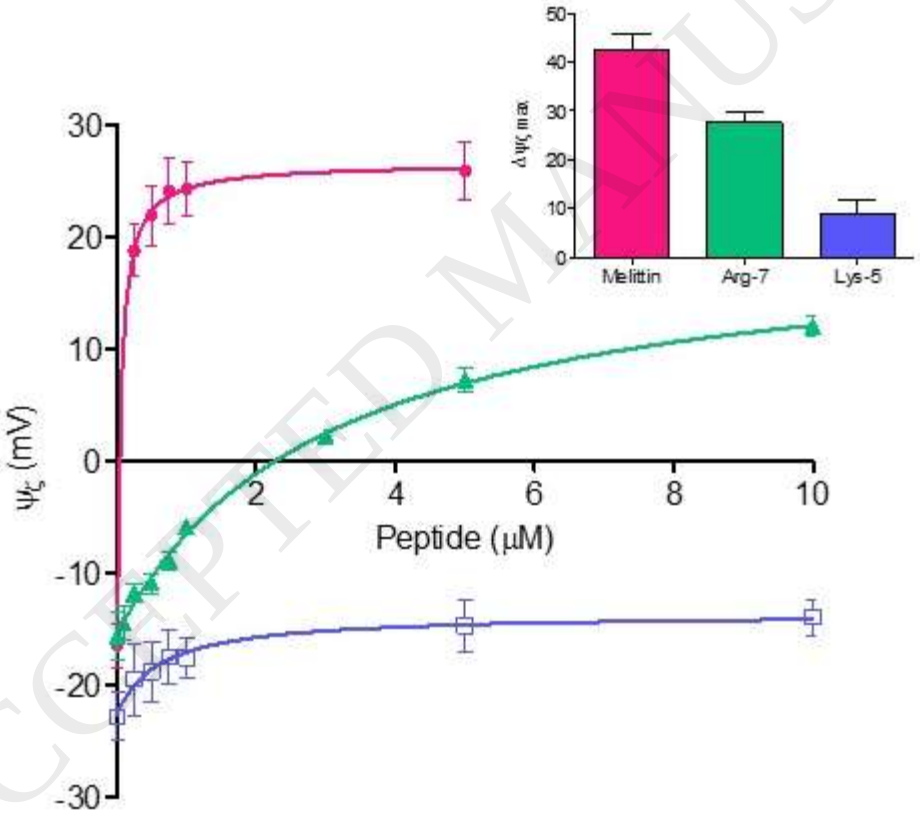

Figure 3. *Change of zeta potential of DMPC liposomes as a function of peptide concentration: ML(●), Arg-7 (▲) and Lys-5 (□). Insert: Maximal effect of peptides on DMPC liposomes zeta potential for the different peptides.*

Figure 4 shows the degree of coverage of these peptides from DMPC membranes, as it was described in material and methods.

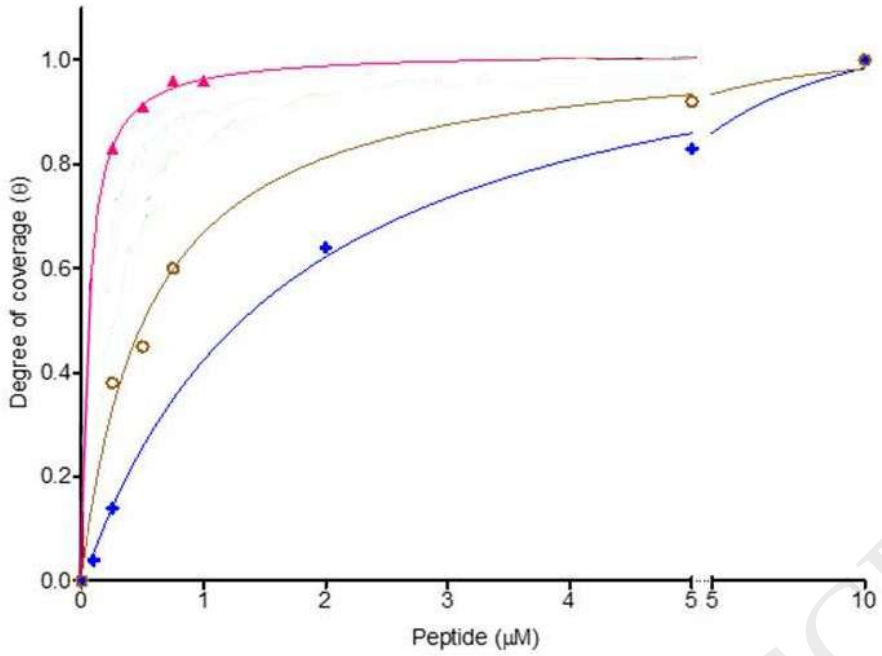

Figure 4. *Adsorption isotherms for MLV of DMPC, at 18ºC: ML (▲), Arg-7 (+), Lys-5 (o)*

The apparent dissociation constant for each type of membrane was estimated from the adsorption curves and there are shown in Table 2. We can appreciate that the binding affinity for ML is higher than those observed for Arg-7 and Lys-5.

Table 2. *Apparent constant dissociation of ML, Arg-7 and Lys-5 for MLV of DMPC al 18ºC*

Lipid	Kd_{app} (µM)	R^2
ML DMPC	0.05 ± 0.01	0.9997
Arg-7 DMPC	1.67 ± 0.24	0.9981
Lys-5 DMPC	0.56 ± 0.10	0.9921

In order to shed light on what happens in these systems at the molecular level, we performed molecular dynamics simulation of 1ML:128 DMPC in water and 1 Lys-5:128 DMPC, as described in Materials and Methods.

The ordering of the system is evaluated here by means of the electron density profile (EDP) normal to the membrane. The profiles were calculated by time averaging the net charge per 0.1 Å thick slabs, assuming a Gaussian distribution centered at the atomic positions with a width of approximately 2 Å.

Figure 5 shows the EDP of the last 250ns (total=300ns) of MD simulations. ML has a slight penetration into the lipid membrane, in comparison with Lys-5 at the same period of simulation time (Figure 5). The same figure shows a different water distribution at membrane interphase with the penetration of ML peptide, while in the case of Lys-5 this effect is not appreciable.

.

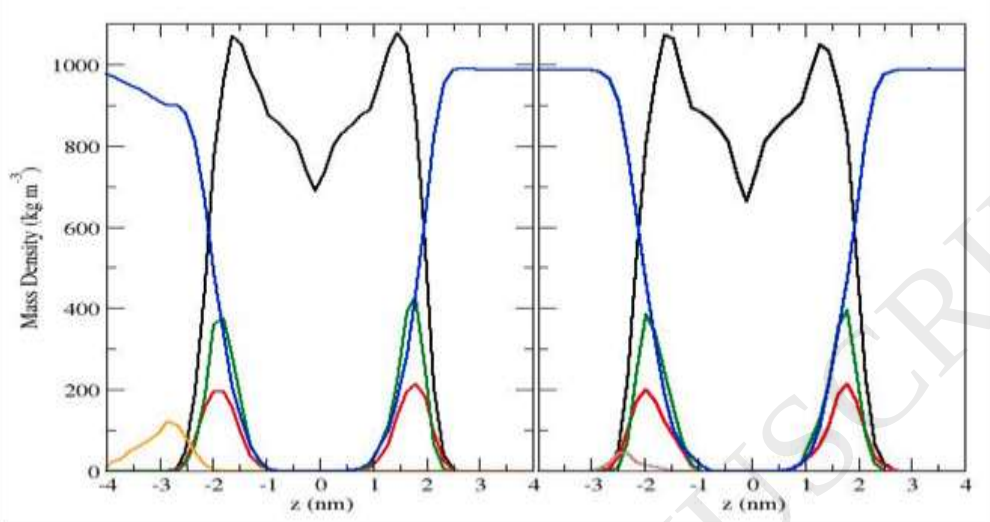

Figure 5. *EDP of MD simulations of 250ns: DMPC (black), water (blue), phosphate groups (green), choline groups (red), ML (orange), Lys-5 (brown).*

At initial simulation time (t=0 ns), the center of mass of the peptides was placed at ~1.5 nm from the bilayer surface. Figure 6 shows one of the most representative snapshots of peptide adsorbing position for the systems of one ML (A) or one Lys-5 (B) with a DMPC bilayer. It is taken for the snapshots of the last 50 ns of 300ns simulation time, that showing the disposition of peptides in the interphasial groups of the lipids. In the case of ML, it is evident a U-shape disposition of the peptide, with at least 3 of the positive net charged exposed to bulk water.

In order to get more detail in these interactions, Figures 6C and D show a higher zoom of green boxes of panels A and B, respectively. In the case of ML, it is possible to observe the hydrogen bonds formed by the amino terminal of ML and the carbonyl oxygen atoms of the lipids, as well as those formed by the NH of the peptide bonds of the amino acids of the C-terminal region and an oxygen atom of phosphate groups or carbonyl groups, as the case may be. The rest of the peptide is evidenced in a U-shape, exposed to the aqueous phase. This ML arrangement would explain the large initial increase in zeta potential to positive values of the ML-DMPC liposomes.

Lys-5 penetrates deeper into the membrane than ML, as shown in Figure 5, and in Figures 6B and D. In this last figure, it can be seen that the Lys residues interact mainly with the phosphate groups of DMPC, according to the smallest increase in zeta potential to positive values.

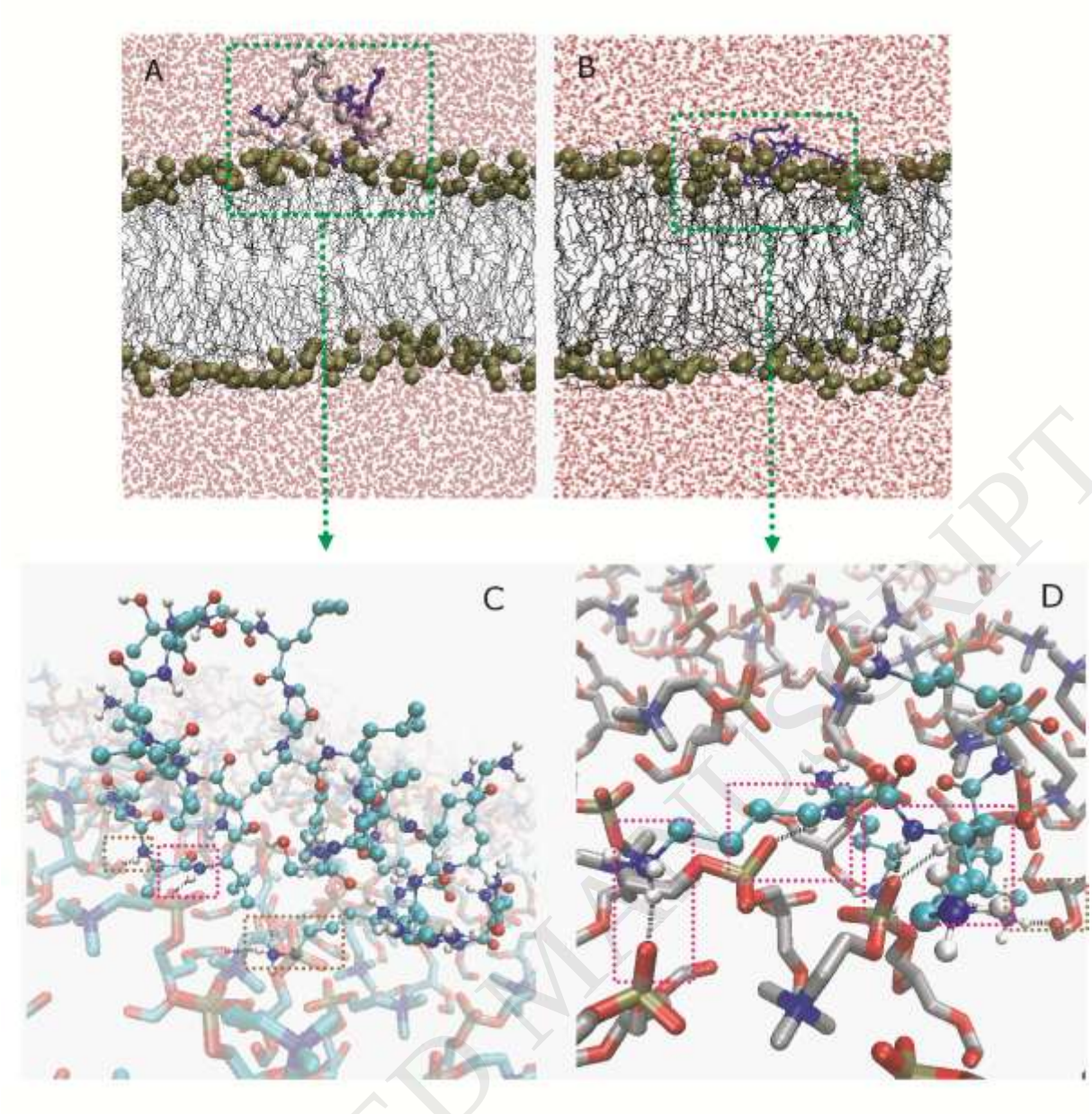

Figure 6. *Snapshots of the most representative position of peptide adsorbing in the systems of one ML (A) or one Lys-5 (B) with DMPC bilayer. Water is represented only by its oxygen atoms (in order to clarify), phosphate atoms are in ochre in VWD representation, the rest of DMPC molecules are in black lines, ML and Lys-5 are in licorice representation, the positive net charged residues are in blue. Green boxes of panels A and B are magnified in panels C and D respectively. They were rotated to evaluate the interaction on the xy plane. Polar headgroups of the lipids are represented in licorice, while peptides are in CPK model. H bonds between lipid headgroups and ML (C) or Lys-5 (D), are in black. Magenta boxes remark H bonds formed by NH of peptide and O carbonylic, while magenta boxes remark H bonds formed by peptide and O of phosphate group. Water molecules and hydrocarbon tails of DMPC were hidden in order to clarify.*

In order to analyze the contribution of net charges to peptide-lipid interaction, Figure 7 shows the interaction energy (E_{int}) of each system: ML:DMPC (Figure 7A) and Lys-5: DMPC (Figure 7B), taking into account the different contributions to this energy: van der Waals and electrostatic components.

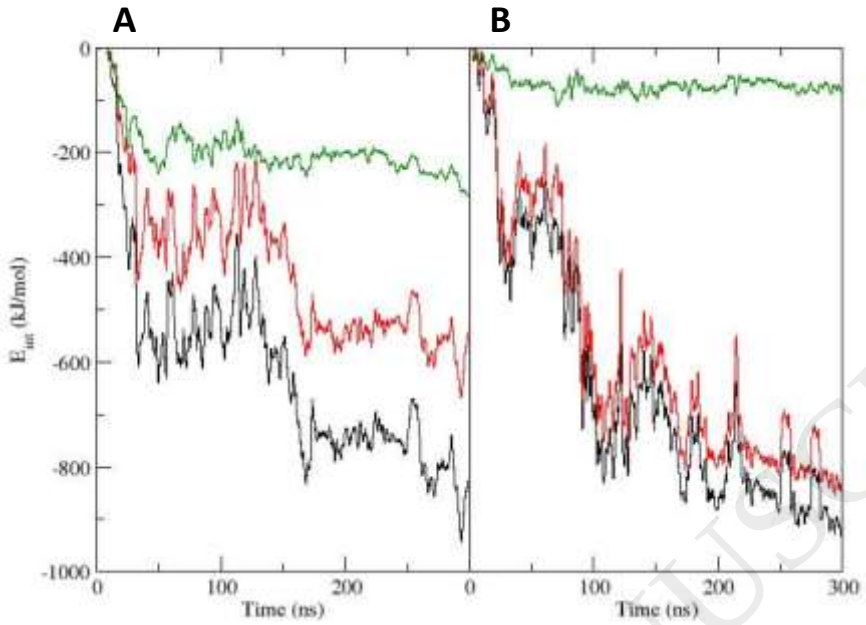

Figure 7. *Interaction energy (E_{int}): total (black), electrostatic contribution (red), van der Waals contribution (green) of:* ***A.*** *ML:DMPC system.* ***B.*** *Lys-5:DMPC system.*

The total E_{int} of both peptides is similar, being higher for ML in the first 150 ns of simulation. Despite this similarity, the different contributions (contributions of charges and short-range forces) are significantly different in both systems. It can be noticed that the main contribution (> 90%) of E_{int} in the Lys-5 system is given by the electrostatic interactions (Figure 7B). In the case of ML (Figure 7A), there is a greater contribution of short-range forces than the previous system. Given that ML has a higher net charge-Lys 5, this realizes ML charges are partly exposed to solvent, without direct interaction with the membrane.

To reinforce this analysis, we study the specific interactions between the principal donors and acceptors of hydrogen bonding groups of both systems.

Figure 8A shows that the running average (each 200ps) of specific interaction in Lys-5 system, increased in the same ratio than ML interactions with lipid bilayer. This figure also shows the number of these H-bonds corresponding to the net charged aminoacids of ML (Arg, Lys and N-terminal). This is in agreement with the previous observation: ML charges are partly exposed to solvent, without direct interaction with the membrane. On the other hand, Lys-5 tends to neutralize the surface charges on the lipid membrane, as we can see in the radial distribution function, [g(r)], between the oxygens of phosphate group and the centre of mass (COM) of ML charged group (black) and Lys-5 (red) (Figure 8B). In the case of Lys-5, all the residues are net charged. Figure 8B shows a closer distribution of Lys-5 to oxygen atoms of phosphate group than ML. The effect on zeta potential seems to be

different for these peptides. Lys-5 residues are closer enough to phosphate group to neutralize phosphate charges, so in this case, the increase in zeta potential is a result of a decrease in negative charges, in relation to existing positive ones (choline groups).

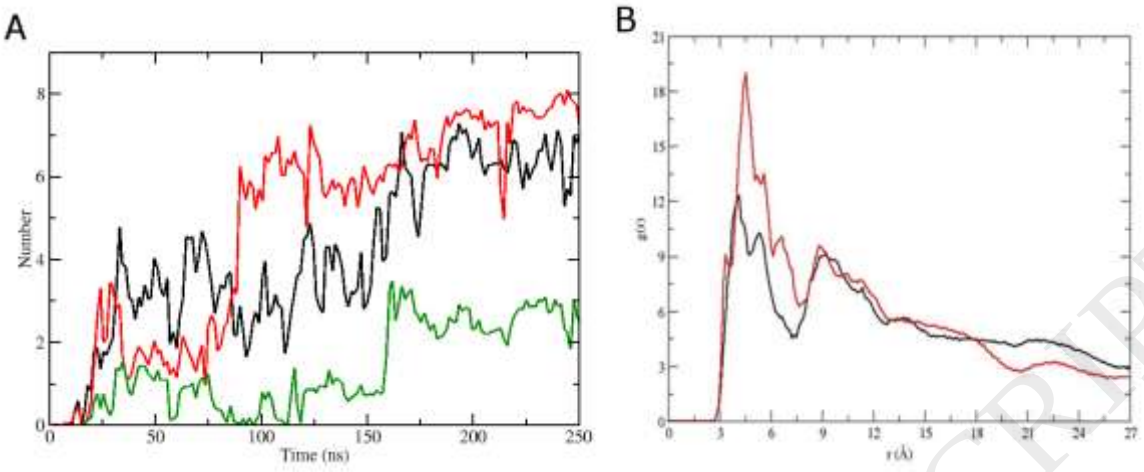

Figure 8. A. *Running average of H bonds interactions each 200 ps, during the production simulation time of: ML (black), Lys-5 (red) and net charged aminoacids of ML (green) with DMPC membrane.* ***B.*** *Radial distribution function of charged residues of ML (black) and Lys-5 (red) in relation to oxygen atoms of phosphate group.*

On the other hand, ML adds positive charges to the surface of the membrane, while it neutralizes some phosphate groups, in the area of interaction (i.e. terminal amino group).

In this sense, the deeper penetration of Lys-5 than ML, and the hairpin configuration of ML, could explain the reach of ML-DMPC to higher zeta potential values than Lys-5-DMPC, in the initial time of the interaction.

Effect of time on the interaction of ML with lipid membranes

From the results discussed above, it could be inferred that the interaction of ML with lipid membrane could be followed by conformational changes or collective interactions. These changes could be dependent of time and ML concentration. Thus, the changes of the ψ_ζ as a time function by ML at different concentrations (0,25; 1 and 5 µM) are compatible with this inference (Figure 9).

The behavior observed in ψ_ζ changes was similar for the different ML concentrations assayed. The ψ_ζ increased during the first 15 min of incubation showing no change during the next 90 min. From this moment and up to 24 hours of incubation with the peptide, the ψ_ζ decreased continually. At short times (the same as at low concentrations: Figure 1) ML interacts with the membrane exposing part of its positive charges to the aqueous phase, which is noticed by the positive changes produced in the zeta potential and the MD simulations of 1 ML peptide. Afterward, there may be a collective behavior of ML peptides or an aggregation and precipitation of MLV's liposomes. However, the turbidimetry, measurements did not show significant changes (data not shown). Therefore, we analyzed

the possibility of collective process of ML peptides.

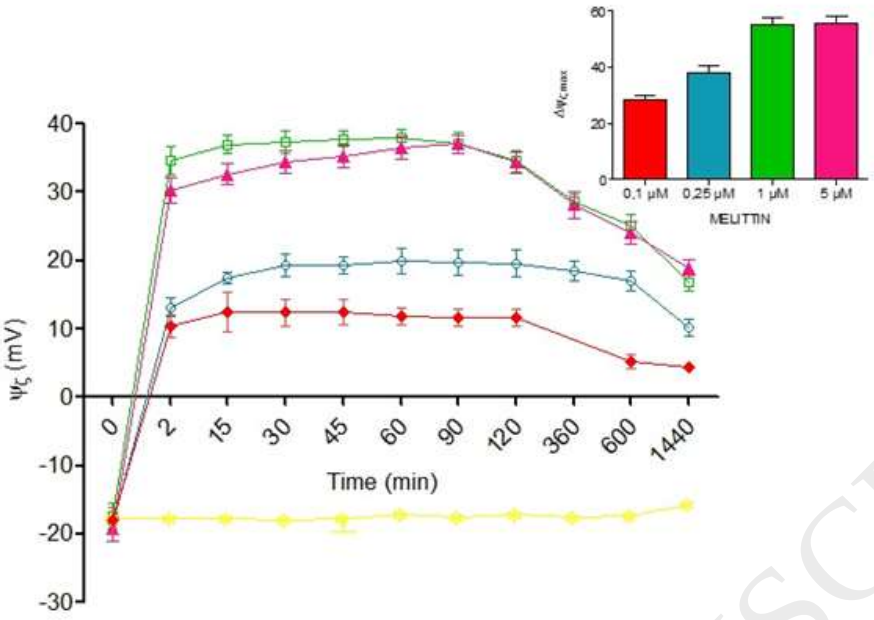

Figure 9. *Change of zeta potential of DMPC liposomes as a function of time: pure DMPC (⋆), in the presence of ML 0,1 (♦), 0,25 (o), 1 (□) and 5 (▲) μM. Insert: Maximal effect of ML on DMPC liposomes zeta potential as a function of time.*

In order to describe at a molecular scale the behavior observed in zeta potential for collective interactions of ML at the different concentrations as a function of time, molecular dynamic simulations were performed. As we were interested in elucidating the collective effects that could be present between ML molecules to organize itself in the membrane, a system of 7 ML in the presence of DMPC lipid bilayer were studied, as described in Material and Methods section. We performed a production run simulation of 600ns.

The evaluation of these simulations shows the formation of two ML clusters, one of them penetrates deeply inside the interphase (Figure S1 of Supplementary Material). With the aim to analyze the perturbation suffered by the membrane, as a consequence of these structures, we evaluated the order parameter of the hydrocarbon chains (*sn1* and *sn2*) of both monolayers of DMPC, at different time periods. The lipid tail order parameter is a standard quantity to evaluate the structural order of acyl chains in lipid bilayers, which can be obtained from deuterium NMR measurements [73]. In MD simulations, it can be determined by:

$$S_{mol} = \frac{1}{2}\left\langle 3\cos^2\theta_n - 1 \right\rangle,$$

where, θ_n is the angle between the normal to the bilayer and the normal to the plane defined by two carbon-deuterium (C-D) bonds in a deuterated n-methylene group of the lipid acyl chain. If UA forcefield is used, as it is our case, the C–D bond vector needs to be reconstructed. In this way, the $C_{(i-1)} - C_{(i+1)}$ vector is usually taken to be the z-axis. The x- and y-axis are defined perpendicular to the z-axis and to each other, with the y-axis in the $C_{(i}$

$_{-1)} - C_{(i)} - C_{(i+1)}$ plane. Using this definition, $S = (2/3)S_{xx}+(1/3)S_{yy}$ and can be compared directly to ^{2}H-NMR data [74,75].

The order parameter is related to the tilt angle of the chains and to the *trans-gauche* distribution of the chain dihedrals, but the relationship is inverse. Figure 10 shows the $-S_{CD}$ order parameters for all lipid methylene groups for *sn*-1 and *sn*-2 DMPC hydrocarbon tails of each monolayer, with and without ML. At the beginning of the interaction, an increase in the order parameter is observed, followed later by an increase in the chain disorder as the peptides penetrate both monolayers.

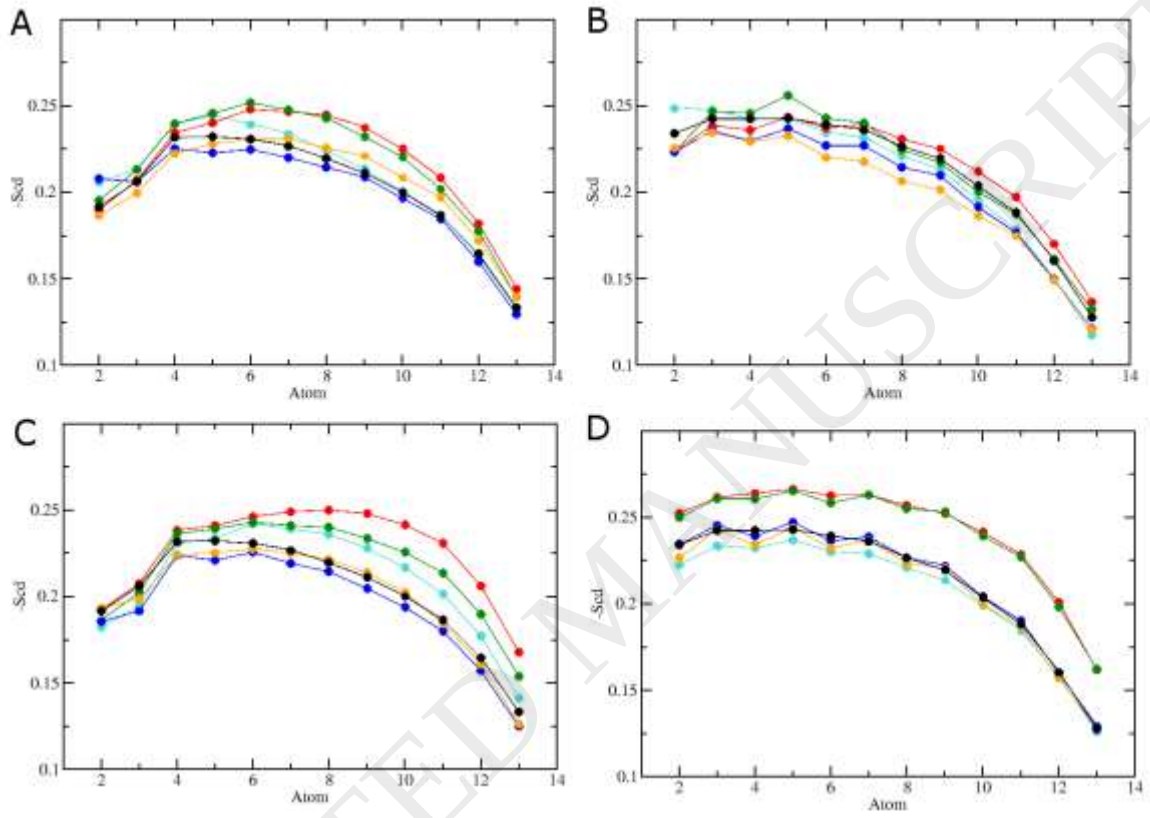

Figure 10. *Order parameters ($-S_{CD}$) as a function of the position of the carbon atoms along the hydrocarbon chain of DMPC sn1 (A-C), sn2 (B-D) for each monolayer of the bilayer. Neat (black), with ML: 100-200 ns (red), 200-300 ns (green), 300-400 ns (cyan), 400-500 ns (orange), 500-600 ns (blue)*

Taking into account this significant change in the wobbling of the hydrocarbon chains of DMPC membrane, it could be suggested that this phenomenon increases the defects that already exist in this ripple membrane phase. For this purpose, we calculated the number of water molecules in the slab of 6 Å width (in z axis) in the middle of the bilayer, as we described in Materials and Methods. This value was determined for a stabilized DMPC membrane (200 ns of productive run) in the absence of ML, and in the study system, DMPC + 7 ML (taking the last 300ns of the simulation). The average value for the case of absence of ML was 1.07 ± 0.09; this value was increased by ~300% (4.2 ± 0.2) in the presence of the peptides (Figure 11).

While this measurement is not an accurate indication that there is a flow of water through the membrane, it suggests an increase in lipid membrane instability, due to the presence of more water molecules inside its structure. On the other hand, the increase in the mobility of the chains is related to an increase in the area per lipid and a closer state to fluid one, in which the zeta potential becomes more negative [76]. This fact would respond to the decrease in the zeta potential as ML peptides get inside the membrane (Figure 9).

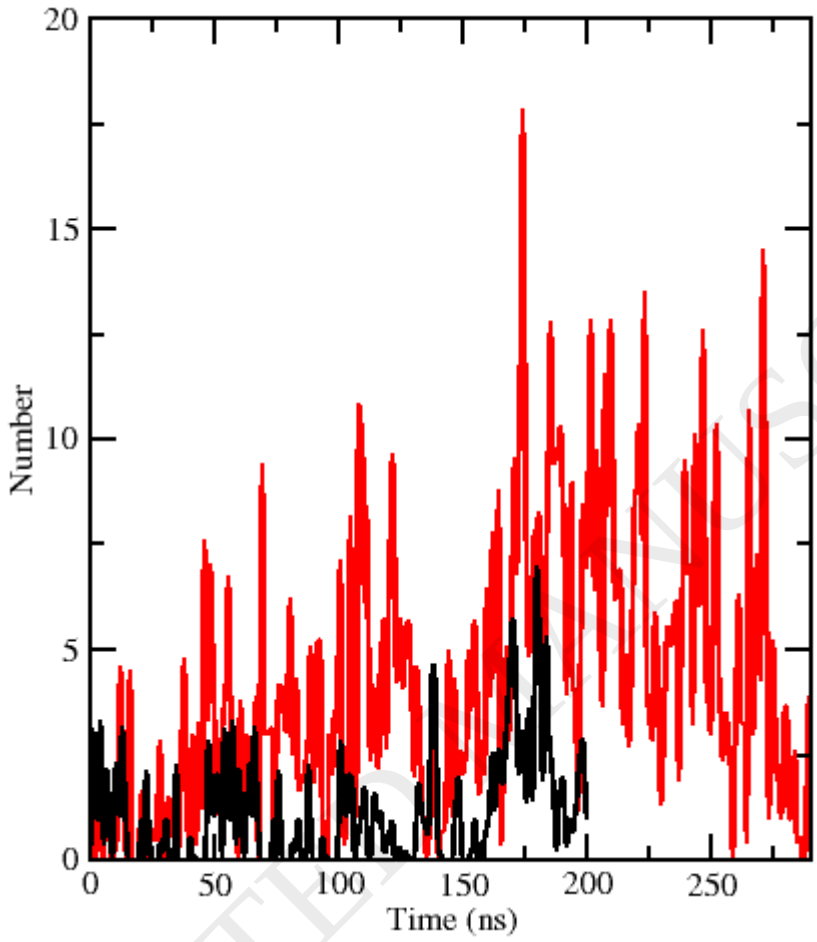

Figure 11. *Running average each 200 ps of number of water molecules in the slab of 6 Å width in the middle of DMPC bilayer in the absence of ML (black) and in the presence of 7 ML (red)*

In order to evaluate a longer simulation time in relation to this system, we assayed a CG type system, under the same conditions as the UA system (already described in Materials and Methods). Its behavior resembles that obtained in the UA systems. Although it is recognized the higher tendency of aggregation of peptides in CG systems of the Martini force field [77], this does not prevent that the aggregated peptides get into the interphase, as they did in the UA system. During the first μs, they are located in the interphase area. At 7μs of simulation, one of the ML separates from the others, and inserted into the hydrocarbon zone with U-shape (Figure 12A).

At ~70μs the peptides separates themselves and form clusters of 2-3 peptides, which penetrate one of the monolayer of the bilayer. The predominant orientation form is with the basic residues interacting with the phosphate groups and the non-polar residues inside the hydrocarbon chains. However, migrations can be observed, both of the polar residues, as

well as those positively charged inside the membrane (Figure 12B and Video S3 in Supplementary Material).

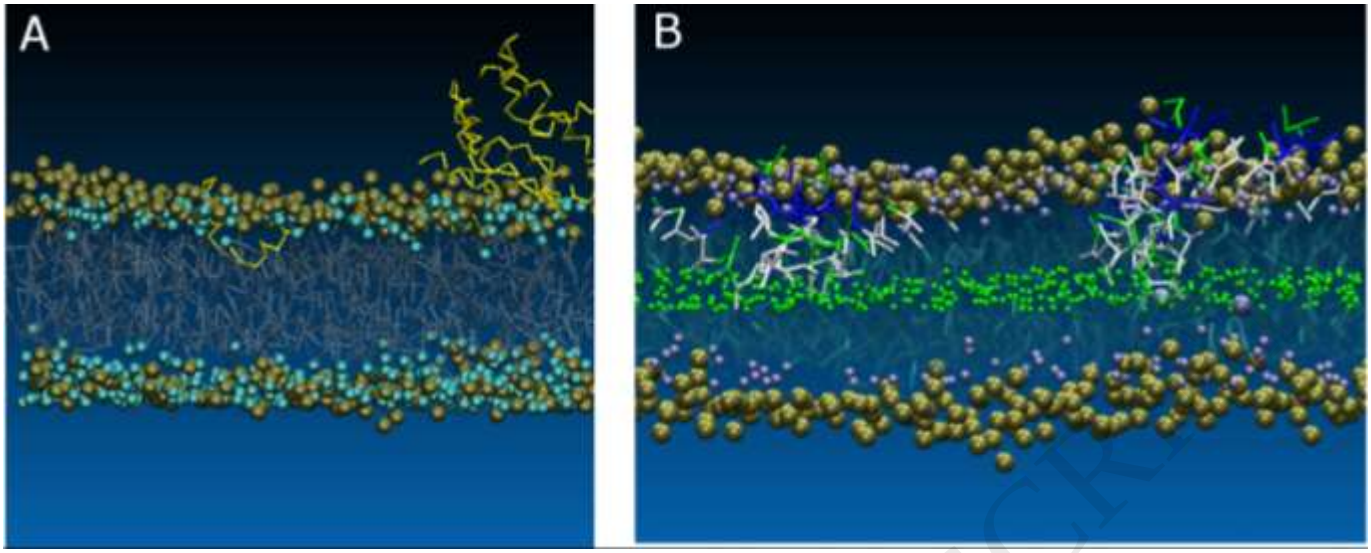

Figure 12. A. *Snapshot at 7.2μs of MD simulation. Phosphate beads are in ochre in VDW representation, hydrocarbon tails in silver licorize, the backbound beads of MLs are in yellow and water between the two interphases of the lipid monolayers are graphed in cyan VDW. Bulk water beads were hidden, in order to clarify.*
B. *Snapshot at 98μs of MD simulation. Phosphate beads are in ochre in VDW representation, hydrocarbon tails in ghost representation, in order to clarify; ML peptides are in licorice representation colored by residue type: apolar residues in white, polar ones in green and positive charged residues in blue. In CPK green representation it is shown the slab of 6Å in the middle of the membrane where water beads were measured. Water beads between the two membrane interphases are represented in purple in CPK representation, the water beads which are in the central slab were represented in VWD. Bulk water beads were hidden, in order to clarify.*

Figure 12B shows 2 clusters of ML with 3 molecules each. There can be seen also the water CG beads inside the bilayer in purple, highlighting in green the center of the membrane.

Regarding these results, and taking into account bibliography already cited, the possibility to form an idealist pore structure in zwiterionic lipid membranes, at the molecular and structural level is subject to assumptions and modes of work mediated by an external force. Of this last way, although the possibility of formation of a pore-like structure at final instance is not discarded, in the first section of the interaction MLs-DMPC, the formation of clusters of between 2 and 3 ML is proposed. These clusters penetrate to reach the central region of the membrane, disturbing both monolayers.

We also calculated in CG systems, the running average each 100ns of the number of water molecules in the slab of 6Å width in the middle of the bilayer, as it was previously described. In the absence of ML, the value was 0.8±0.1, similar to that obtained at UA level, and in the presence of ML the value increased by ~400% (4.9 ± 0.1). It is important to remark that each water CG bead represent 4 water molecules. Although these structures that stabilize in the monolayer do not represent the traditional pore structure, they do manifest a considerable permeation of water through the membrane without complete break of it – in agreement with no changes in turbidimetry assays –, but changing its surface properties.

CONCLUSIONS

The variations of the zeta potential in membranes of DMPC at 18ºC by the presence of ML, allow us to clarify the knowledge of the mechanism of action of this peptide, at least in the first stages of the interaction.

A molecular approach through MD simulations allows us to determine that the significant increase in potential was mainly due to the exposure of positive charges to the aqueous phase, at low ML concentrations or at low times. When the concentration of ML increases (or the time increases), more peptide molecules reach the surface of the liposomes. A collective effect of ML favors the penetration of peptide molecules into a monolayer of the lipid bilayer. These structures are formed by 2 or 3 ML peptides and show important changes in the properties of the membrane, especially in the arrangement of their hydrocarbon chains, which determines an increase in water permeability, possibly mediated by an increase in defects found at the interphase of the membrane in Pβ phase.

Although the formation of these structures does not rule out the possibility of pore formation in later instances, they open the way to the understanding of the mechanism by which the ML begins its action in zwitterionic membranes. These effects are sufficiently disturbing of the properties of the target membrane, to promote an increase of the presence of water inside the membrane up to 400%, as reached in the last μs of the simulation.

Taking into account that in high doses, melittin may cause itching, inflammation, and local pain, and on the other hand, small doses of melittin produce anti-inflammatory effects [78], and the majority of the desired pharmacological effects; the potential technical developments of nanostructured lipid systems would be helpfull to modify this toxic peptide into a safe therapeutic agent. [79]. The physicochemical and molecular knowledge of the interaction between this peptide and the lipid systems allows us to bring near the development of release systems, with techniques that modulate phase states, as is the case, for example, of the modulation of lipid membrane curvature. [80,81].

Acknowledgements

This work was supported by funds from Agencia Nacional de Promoción Científica y Tecnológica, grant PICT-2011-2606 and PICT-2014-3653.
EAD, MFM and ACC are members of the Research Career of CONICET (Consejo Nacional de Investigaciones Científicas y Técnicas de la República Argentina).
MJET is a PhD student with a CONICET scholarship.

References

[1] H.J. Park, S.H. Lee, D.J. Son, K.W. Oh, K.H Kim, H.S. Song, G.J. Kim, G.T. Oh, D.Y. Yoon and J.T. Hong,Antiarthritic effect of bee venom: inhibition of inflammation mediator generation by suppression of

NF-kappaB through interaction with the p50 subunit. Arthritis Rheum, 50 (11) (2004) 3504–3515.DOI 10.1002/art.20626

[2] D.J. Son , J.W. Lee, Y.H. Lee, H.S. Song, C.K. Lee and J.T. Hong, Therapeutic application of anti-arthritis, pain-releasing, and anti-cancer effects of bee venom and its constituent compounds. Pharmacology & Therapeutics, 115 (2007) 246-270.

[3] E. Habermann, Bee and wasp venoms. Science, 177 (1972) 314–322.DOI: 10.1126/science.177.4046.314

[4] E. Habermannand J. Jentsch, Sequenzanalyse des Melittinsaus den tryptischen und peptischenSpaltstucken. Hoppe-Seyler´s Z. Physiol. Chem., 348 (1967) 37-50.

[5] B. Bechinger, Structure and Functions of Channel-Forming Peptides: Magainins, Cecropins, Melittin and Alamethicin. J.Membr Biol., 156 (3) (1997) 197–211.

[6] K. Matsuzaki, S. Yoneyama and K. Miyajima, Pore Formation and Translocation of Melittin. Biophys. J., 73 (1997) 831-838.

[7] H. Raghuraman and A. Chattopadhyay,Melittin: a membrane-active peptide with diverse functions. Biosci Rep., 27 (2007) 189–223.

[8] S. Huang, J. Wang, X. Wang and C. Li,Melittin: A Key Composition of Honey Bee Venom with Diverse Pharmaceutical Function. Advances in Biological Sciences Research, 3 (2017) 193-197.

[9] C.R. Dawson, A.F. Drake, J. Helliwell and R.C. Hider, The interaction of bee melittin with lipid bilayer membranes. Biochim.Biophys.Acta, 510 (1978) 75-86.

[10] W.F. De Grado, G.F. Musso, M. Lieber, E.T. Kaiser and F.J. Ktzdy, Kinetics and mechanism of hemolysis induced by melittin and by a synthetic melittin analogue. Biophys. J., 37(1982) 329-338.

[11] C. Dempsey, R. Bazzo and I.D. Campbell, Conformational dynamics of melittin and [ala-14]-melittin by NMR and amide exchange, and significance for melittins membrane-activities. Biophys. J., (1990) 57-76.

[12] P.J. Russell, D. Hewish, T. Carter, K. Sterling-Levis, K. Ow, M. Hattarki, L. Doughty, R. Guthrie, D. Shapira, P.L. Molloy, J.A. Werkmeister and A.A. Kortt, Cytotoxic properties of immunoconjugates containing melittin-like peptide 101 against prostate cancer: in vitro and in vivo studies. Cancer ImmunolImmunother, 53 (2004) 411–421.

[13] G. Gajski and V. Garaj-Vrhovac,Melittin: A lytic peptide with anticancer properties. Environ ToxicolPharmacol., 36 (2013) 697–705.

[14] B. Bechinger, The structure, dynamics and orientation of antimicrobial peptides in membranes by nultidimensional solid-state NMR spectroscopy. Biochim.Biophys. Acta,1462 (1999) 157-183.

[15] H.W. Huang, Action of antimicrobial peptides: two-state model. Biochemistry, 39 (2000) 8347–8352.

[16] Y. Shai, Mode of action of membrane active antimicrobial peptides. Biopolymers, 66 (2002) 236–248.

[17] D. Allende, S.A. Simon and T.J. McIntosh,Melittin-induced bilayer leakage depends on lipid material properties: evidence for toroidal pores. Biophys. J., 88 (2005) 1828–1837.

[18] K. Hristova, C.E Dempsey and S.H. White, Structure, location, and lipid perturbations of melittin at the membrane interface. Biophys. J., 80(2001) 801–811.

[19] L. Yang, T.A. Harroun, T.M. Weiss, L. Ding and H.W. Huang, Barrel-Stave Model or Toroidal Model? A Case Study on Melittin Pores. Biophys. J., 81 (2001) 1475–1485.

[20] P.F.Almeida and A. Pokorny, Mechanisms of antimicrobial, cytolytic, and cell-penetrating peptides: from kinetics to thermodynamics. Biochemistry, 48 (2009) 8083–8093.

[21] G. Van den Bogaart, J.V. Guzman, J.T. Mika and B. Poolman, On the mechanism of pore formation by melittin. J.BiolChem, 283 (2008) 33854–33857.

[22] K.P. Santo, S.J. Irudayam and M.L. Berkowitz, Melittin Creates Transient Pores in a Lipid Bilayer: Results from Computer Simulations, J. Phys. Chem. B, 117 (17) (2013), 5031–5042

[23] L.R. Brown, J. Lauterwein and K.Wuthrich, High-resolution 1HNMR studies of self-aggregation of melittin in aqueous solution. Biochim.Biophys. Acta, 622 (1980) 231–244.

[24] M. Iwadate, T.Asakura and M.P. Williamson, The structure of the melittin tetramer at different temperatures—an NOE-based calculation with chemical shift refinement. Eur J Biochem, 257 (1998) 479–487.

[25] L. Zhu, M.D. Kemple, P. Yuan and F.G. Prendergast, N-terminus and lysine side chain pKa values of melittin in aqueous solutions and micellar dispersions measured by 15 N NMR. Biochemistry, 34 (1995)13196–13202

[26] A.S. Ladokhin and S.H. White,`Detergent-like' permeabilization of anionic lipid vesicles by melittin. Biochim.Biophys. Acta, 1514 (2001) 253-260.

[27] N. Papo N. and Y. Shai, Exploring Peptide Membrane Interaction Using Surface Plasmon Resonance: Differentiation between Pore Formation versus Membrane Disruption by Lytic Peptides. Biochemistry, 42 (2003) 458-466.

[28] S.J. Irudayamand M.L. Berkowitz, Influence of the arrangement and secondary structure of melittin peptides on the formation and stability of toroidal pores. Biochim.Biophys. Acta, 1808 (2011) 2258–2266.

[29] H.W. Huang, Molecular mechanism of antimicrobial peptides: the origin of cooperativity. Biochim. Biophys. Acta, 1758 (2006) 1292–1302.

[30] M. Manna and C.Mukhopadhyay, Cause and effect of melittininduced pore formation: a computational approach. Langmuir, 25 (2009) 12235–12242.

[31] Y. Lyu, N. Xiang, X. Zhu and G.Narsimhan, Potential of mean force for insertion of antimicrobial peptide melittin into a pore in mixed DOPC/DOPG lipid bilayer by molecular dynamics simulation. Journal of Chemical Physics, 146(15) (2017) 155101.

[32] D. Sun, J. Forsman and C.E. Woodward, Molecular Simulations of Melittin-Induced Membrane Pores. J. Phys Chem B, 121(44) (2017) 10209-10214.

[33] K.P. Santo, S.S. Irudayam and M.L. Berkowitz. Melittin creates transient pores in a lipid bilayer: Results from computer simulations. J. Phys Chem B, 117 (2013) 5031–5042.

[34] S.K. Upadhyay, Y. Wang, T. Zhao and J.P.Ulmschneider, Insights from Micro-second Atomistic Simulations of Melittin in Thin Lipid Bilayers. J.Membr Biol., 248(3) (2015) 497-503.

[35] R. Koynova and M.Caffrey, Phases and phase transitions of the phosphatidylcholines, Biochim.Biophys. Acta, 1376 (1998) 91–145.

[36] J. Lee, S.W. Jung, A.E. Cho, Molecular Insights into the Adsorption Mechanism of Human β-Defensin-3 on Bacterial Membranes, Langmuir, 32 (7), (2016) 1782-1790.

[37] T. Heimburg, A model for the lipid pretransition: coupling of ripple formation with the chain-melting transition. Biophys. J., 78(3) (2000) 1154–1165.

[38] U. Bernchou, H. Midtiby, J. Hjort Ipsen, A. Cohen Simonsen, Correlation between the ripple phase and stripe domains in membranes. BBA (Biomembranes) 1808 (2011) 2849-2858

[39] C. Almeida, A. Lamazière, A. Filleau, Y. Corvis, P. Espeau, J. Ayala-Sanmartin, Membrane re-arrangements and rippled phase stabilisation by the cell penetrating peptide penetratin. BBA (Biomembranes) 1858 (2016) 2584-2591

[40] Kumar A., Dahl V., Kleinen J., Gambaryan-Roisman T., Venzmer J., Influence of lipid bilayer phase behavior and substrate roughness on the pathways of intact vesicle deposition: A streaming potential

study, Colloids and Surfaces A: Physicochem. Eng. Aspects 521 (2017) 302–311

[41] A.D. Bangham, J.O. de Gier and G.D. Greville,Osmotic properties and water permeabilityof phospholipid liquid crystals. Chem. Phys. Lipids., 1 (1967) 225–246.

[42] A.D. Bangham, M.W. Hill and N.G.A. Miller, Preparation and use of liposomes as models of biological membranes In “Methods in membrane biology”, E.D. Korn(Ed) Plenum Press, New York, 1974; chapter1, pp 1-68.

[43] H.H. Hess and J.E. Derr, Assay of inorganic and organic phosphorus in the 0.1-5 nanomole range. Anal.Biochem., 63 (1975) 607–613.

[44] P.S. Chen, T.Y. Toribara and H. Warner, Micro determination of phosphorus. Anal. Chem., 28 (1956) 1756–1758.

[45] B.N Ames, Assay of inorganic phosphate, total phosphate and phosphatases. Methods Enzymol., 8 (1966) 115–118.

[46] M.T. Lee, T.L. Sun, W.C. Hung and H.W. Huang,Process of inducing pores in membranes by melittin. Proc. Natl. Acad. Sci. USA, 110 (2013) 14243–14248.

[47] H. Vogel and F.Jahnig, The structure of melittin in membranes. Biophys. J., 50 (1986) 573–582.

[48] D. Sengupta, H.Leontiadou, A.E. Mark and S.J.Marrink, Toroidal Pores Formed by Antimicrobial Peptides Show Significant Disorder. Biochim. Biophys. Acta, 1778 (2008) 2308-2317.

[49] M.J. Abraham, D. van der Spoel, E. Lindahl, B. Hess and the GROMACS development team (2014) GROMACS User Manual version 5.0.4, www.gromacs.org

[50] H.J.C. Berendsen, D. van der Spoel and R. van Drunen, GROMACS: A message-passing parallel molecular dynamics implementation, In Computer Physics Communications, 91 (1–3) (1995) 43-56, ISSN 0010-4655.

[51] E. Lindahl, B. Hess and D. van der Spoel, GROMACS 3.0: a package for molecular simulation and trajectory analysis. J. Mol. Model, 7 (2001) 306.

[52] D. van der Spoel, E. Lindahl, B. Hess, G. Groenhof, A.E. Mark and H.J. Berendsen, GROMACS: fast, flexible, and free. J. Comput. Chem, 26 (2005) 1701-1718.

[53] B. Hess, C. Kutzner, D. van der Spoel and E. Lindahl, GROMACS 4: Algorithms for Highly Efficient, Load-Balanced, and Scalable Molecular Simulation. Journal of Chemical Theory and Computation, 4 (3) (208) 435-447. DOI: 10.1021/ct700301q.

[54] S. Pronk, S. Páll, R. Schulz, P. Larsson, P. Bjelkmar, R. Apostolov, M.R. Shirts, J.C. Smith, P.M. Kasson, D. van der Spoel, B. Hess and E. Lindahl, GROMACS 4.5: a high-throughput and highly parallel open source molecular simulation toolkit. Bioinformatics, 29(7) (2013) 845-54. doi: 10.1093/bioinformatics/btt055.

[55] M.J. Abraham, T. Murtola, R. Schulz, S. Páll, J.C. Smith, B. Hess and E. Lindahl, GROMACS: High performance molecular simulations through multi-level parallelism from laptops to supercomputers, SoftwareX, 1–2 (2015) 19-25.

[56] C. Oostenbrink, A. Villa, A.E. Mark and W.F. Van Gunsteren, A biomolecular force field based on the free enthalpy of hydration and solvation: the GROMOS force-field parameter sets 53A5 and 53A6.J. Comput. Chem., 13 (2004) 1656-76.

[57] I. Chandrasekhar, M. Kastenholz, R.D. Lins, C. Oostenbrink, L.D. Schuler, D.P. Tieleman and W.F. van Gunsteren, A consistent potential energy parameter set for lipids: dipalmitoylphosphatidylcholine as a benchmark of the GROMOS96 45A3 force field. Eur. Biophys. J., 32 (2003) 67-77.

[58] O. Berger, O. Edholm and F. Jähnig, Molecular dynamics simulations of a fluid bilayer of

dipalmitoylphosphatidylcholine at full hydration, constant pressure, and constant temperature. Biophys. J., 72(5) (1997) 2002-2013.

[59] H.J.C. Berendsen, J.P.M. Postma, W.F. van Gunsteren and J. Hermans, Interaction models of water in relation to protein hydration. In Intermolecular forces: Proceedings of the Fourteenth Jerusalem Symposium on Quantum Chemistry and Biochemistry, B. Pullman (Ed), 1981, 331-342, Reidel Publ. Company, Dordrecht, Holland.

[60] T. Darden, D. York and L. Pedersen, Particle mesh Ewald: An N·log(N) method for Ewald sums in large systems. J. Chem. Phys., 98 (12) (1993) 10089-10092.

[61] U. Essmann, L. Perera, M.L. Berkowitz, T. Darden, H. Lee and L.G. Pedersen, A smooth particle mesh Ewald method. J. Chem. Phys., 103 (19) (1995) 8577-8593.

[62] D.H. De Jong, G. Singh, W.F.D. Bennet, C. Arnarez, T.A. Wassenaar, L.V. Schafer, X. Periole, D.P. Tieleman and S.J. Marrink, Improved Parameters for the Martini Coarse-Grained Protein Force Field. J. Chem. Theory Comput., (2012) DOI: 10.1021/ct300646g.

[63] L. Monticelli, S. Kandasamy, X. Periole, R. Larson, D.P. Tieleman and S.J. Marrink, The MARTINI coarse grained force field: extension to proteins. J. Chem. Theory Comput., 4 (2008) 819-834.

[64] S.J. Marrink, H.J. Risselada, S. Yefimov, D.P. Tieleman and A.H. de Vries, The MARTINI forcefield: coarse grained model for biomolecular simulations. J. Phys. Chem. B, 111 (2007) 7812-7824.

[65] S.J. Marrink, A.H. de Vries and A.E. Mark,Coarse grained model for semi-quantitative lipid simulations. J. Phys. Chem. B, 108 (2004) 750-760.

[66] T.A. Wassenaar, H.I. Ingólfsson, R.A. Böckmann, D.P. Tieleman and S.J. Marrink, Computational lipidomics with insane: a versatile tool for generating custom membranes for molecular simulations. J. Chem. Theory Comput., 11 (2015) 2144–2155.

[67] A.H. de Vries, S. Yefimov, A.E. Mark, and S.J. Marrink. Molecular structure of the lecithin ripple phase. PNAS 102 (2005) 5392–5396.

[68] W. Humphrey, A. Dalke and K. Schulten, VMD: Visual molecular dynamics. J. Mol. Graph., 14 (1) (1996) 33-38, https://doi.org/10.1016/0263-7855(96)00018-5.

[69] M.F. Martini and E.A. Disalvo, Superficially active water in lipid membranes and its influence on the interaction of an aqueous soluble protease. Biochim. Biophys. Acta, 1768 (10) (2007) 2541-2548.

[70] A.M. Bouchet, M.A. Frías, F. Lairion, F. Martini, H. Almaleck, G. Gordillo and E.A. Disalvo, Structural and dynamical surface properties of phosphatidylethanolamine containing membranes. Biochim. Biophys. Acta,1788 (5) (2009) 918-925.

[71] M.F. Martini and E.A. Disalvo, Influence of electrostatic charges and non electrotatic components on the adsorption of an aspartyl protease on lipid bilayers. Colloids Surf. B Biointerfaces, 22 (3) (2001) 219-226.

[72] M.F. Martini and E.A. Disalvo, Effect of polar head groups on the activity of aspartyl protease adsorbed to lipid membranes. Chem. Phys. Lipids, 122 (2003) 177-183.

[73] A. Seelig and J. Seelig, J. Biochem. , 1974, 13, 4839-4845.

[74] E. Egberts, S.-J. Marrink, H.J.C. Berendsen, Eur. Biophys. J. , 1994, 22, 423-436

[75] L.S. Vermeer, B.L. de Groot, V. Reat, A. Milon and J. Czaplicki, Eur. Biophys. J. , 2007, 36, 919–931

[76] M.A. Morini, M.B. Sierra, V.I. Pedroni, L.M. Alarcon, G.A. Appignanesi and E.A. Disalvo, Influence of temperature, anions and size distribution on the zeta potential of DMPC, DPPC and DMPE lipid vesicles, Colloids Surf. B Biointerfaces, 131 (2015) 54–58.

[77] M. Javanainen, Excessive aggregation of membrane proteins in the Martini model. PLoS One,(2017) 12(11): e0187936.

[78] Raghuraman, H.; Chattopadhyay, A. Melittin: A membrane-active peptide with diverse functions. Biosci. Rep. 2007, 27, 189–223.

[79] Lee G. and Bae H. Anti-Inflammatory Applications of Melittin, a Major Component of Bee Venom: Detailed Mechanism of Action and Adverse Effects, Molecules 2016, 21, 616-626.

[80] Girona v., Domènech O., Prat J., Ortiz A., Muñoz-Juncosa M. M., Pujol M., Characterization and lipid phase effect on the interaction of GBV-C E2-derived peptide, P6-2VIR576, with lipid membranes relating it with the HIV-1 FP inhibition, Colloids and Surfaces A 554 (2018) 187–196

[81] Lasoń E., Sikora E., Miastkowska M., Socha P., Ogonowski J., NLC delivery systems for alpha lipoic acid: Physicochemical characteristics and release study, Colloids and Surfaces A 532 (2017) 57–62